Vincent, J. P., Cavey, D., Kamenka, J. M., Geneste, P., & Lazdunski, M. (1978) *Brain Res. 152*, 176-182.
Vincent, J. P., Karalovski, K., Geneste, P., Kamenka, J. M., & Lazdunski, M. (1979) *Proc. Natl. Acad. Sci. U.S.A. 76*, 4678-4682.
Zukin, R. S., & Kream, R. M. (1979) *Proc. Natl. Acad. Sci. U.S.A. 76*, 1593-1597.
Zukin, R. S., & Zukin, S. R. (1981) *Life Sci. 29*, 2681-2690.
Zukin, S. R., & Zukin, R. S. (1979) *Proc. Natl. Acad. Sci. U.S.A. 76*, 5372-5376.
Zukin, S. R., Young, A. B., & Snyder, S. H. (1974) *Proc. Natl. Acad. Sci. U.S.A. 71*, 4802-4807.
Zukin, S. R., Fitz-Syage, M. L., Nichtenhauser, R., & Zukin, R. S. (1983) *Brain Res. 258*, 277-284.
Zukin, S. R., Bardy, K. T., Slifer, B. L., & Bolster, R. L. (1984) *Brain Res. 294*, 174-177.

Four- and Five-Coordinate Species in Nickel-Reconstituted Hemoglobin and Myoglobin: Raman Identification of the Nickel-Histidine Stretching Mode†

John A. Shelnutt*
Solid State Materials Division, Sandia National Laboratories, Albuquerque, New Mexico 87185
Kenneth Alston
Department of Natural Sciences, Benedict College, Columbia, South Carolina 29204
Jui-Yuan Ho and Nai-Teng Yu
School of Chemistry, Georgia Institute of Technology, Atlanta, Georgia 30332
Tomoko Yamamoto
Laboratory of Chemical Physics, National Institute of Arthritis, Diabetes, and Digestive and Kidney Diseases, National Institutes of Health, Bethesda, Maryland 20205
Joseph M. Rifkind
Laboratory of Cellular and Molecular Biology, Gerontology Research Center, National Institute on Aging, National Institutes of Health, Baltimore, Maryland 21224
Received May 15, 1985

ABSTRACT: Nickel(II)-reconstituted hemoglobin (^{Ni}Hb) and myoglobin (^{Ni}Mb) and model Ni porphyrins have been investigated by Soret-resonance Raman difference spectroscopy. Two sets of frequencies for the oxidation-state and core-size marker lines in the region from 1300 to 1700 cm^{-1} indicate two distinct sites in ^{Ni}Hb. Only one of these sites is evident in the Raman spectra of ^{Ni}Mb. This result is consistent with the UV-visible absorption spectrum of ^{Ni}Hb, which shows two Soret bands at 397 and 420 nm and one Soret at 424 nm for ^{Ni}Mb. Excitation at the blue Soret component of ^{Ni}Hb with 406.7-nm laser radiation preferentially enhances the set of Raman marker lines typical of Ni-protoporphyrin IX [Ni(ProtoP)] in noncoordinating solvents. The wavelength of the blue Soret component and the Raman spectrum indicate four-coordination for this site in ^{Ni}Hb. Laser excitation in the red Soret band enhances a set of lines whose frequencies are compatible with neither four- nor six-coordinate frequencies but are intermediate between the two. The red Soret band of the proteins is also considerably less red shifted than six-coordinate Ni-porphyrin models. These results suggest that Ni in the second site possesses a single axial ligand. Raman spectra of ^{64}Ni-reconstituted and natural abundance Ni-reconstituted hemoglobins, obtained simultaneously in a Raman difference spectrometer, have identified the Ni-ligand stretch at 236 cm^{-1}. The line shifts to 229 cm^{-1} for the ^{64}Ni-reconstituted Hb. For a pure Ni-ligand stretch a 10-cm^{-1} shift would be predicted. A decrease of almost 7 cm^{-1} indicates a high degree of Ni-ligand character for the assigned mode. The frequency of the Ni-ligand stretch, falling as it does in the range of Fe-histidine stretching frequencies, points to histidine as the axial fifth ligand. The frequency of the Ni-histidine mode is slightly higher than that for the Fe-histidine mode in hemoglobin but lower than that observed for horseradish peroxidase. We find that the Ni-histidine mode is 5 cm^{-1} higher in ^{Ni}Mb (R-like) than in ^{Ni}Hb (T structure). A similar increase in the Fe-histidine frequency is noted in the comparison of the native deoxy proteins. The Raman results show that the local structural changes associated with a change in quaternary structure are the same at the metal site for both Ni-reconstituted and Fe hemoglobins.

Catalysis, ligand binding, redox reactions, and light to chemical energy transduction are among the important functions of metalloporphyrin-containing proteins in biology. Analogous biomimetic chemistries are also of current interest. To further develop and understand these chemistries, a detailed understanding of the relationship between protein structure and metalloporphyrin reactivity for this class of proteins would be useful.

One method of investigating structure-reactivity relationships is by making a comparison of systematically modified enzymes. Recently, a variety of transition metals have been substituted for iron in the central core of the porphyrin ring

† This work was supported by U.S. Department of Energy Contract DE-AC04-76-DP00789 and Gas Research Institute Contract 5082-260-0767.

0006-2960/86/0425-0620$01.50/0

of several heme proteins including cytochrome *c*, hemoglobins, and myoglobin (Flatmark & Robinson, 1968; Hoffman, 1979; Alston & Storm, 1979). These metal-substituted heme proteins offer an important new method of investigating the role of the metal ion in catalytic and ligand-binding functions of heme proteins.

Recent work (Alston et al., 1980, 1982, 1984, 1985; Manoharan et al., 1983, 1985) on metal-reconstituted hemoglobin (Hb) and myoglobin (Mb) reveal a number of interesting features of the metal's interaction with the protein and with the porphyrin ring itself. In particular, the work with nickel- and copper-reconstituted hemoglobins (^{Ni}Hb and ^{Cu}Hb) offers novel insights into the relationship between the quaternary structure of the Hb subunits and the local structure at the heme active site. ^{Ni}Hb and ^{Cu}Hb do not bind oxygen in contrast to the iron and cobalt hemoglobins, but these metals serve well as reporters of structural changes at the metal.

Spectroscopic and chemical studies (Alston et al., 1980, 1982, 1984, 1985; Manoharan et al., 1983, 1985) show the subunits of Ni- and Cu-modified Hb to be in the deoxy or T structure. Treatment with carboxypeptidase A (CPA) modifies the contacts between subunits at a location far from the metalloporphyrin; the spectra and sulfhydryl group reactivity measurements indicate a change from the T structure to the oxy or R structure. The CPA-induced quaternary structure change results in changes at the active site of the reconstituted and native hemoglobins.

UV–visible absorption and electron paramagnetic resonance (EPR) spectra of the Ni and Cu hemoglobins indicate the metalloporphyrin in each of the four subunits occupies one of two distinct sites (Manoharan et al., 1985). Upon CPA conversion, ^{Ni}Hb and ^{Cu}Hb switch to a structure that possesses only one of the two spectroscopically distinct sites, namely, the site similar to that observed for Ni- and Cu-reconstituted myoglobin (^{Ni}Mb and ^{Cu}Mb).

UV–visible and EPR results are consistent with the Ni(II) ion in ^{Ni}Mb and CPA–^{Ni}Hb being five-coordinate, i.e., possessing only one axial ligand. In the T structure, the Ni and Cu hemoglobins exhibit the putative five-coordinate form and also another form thought to be either six-coordinate with two weak axial ligands or four-coordinate with no axial ligands (Manoharan et al., 1985).

Resonance Raman spectroscopy has proved useful in addressing questions of the state of ligation and aggregation of the Cu–porphyrin in copper-modified cytochrome *c* (^{Cu}cyt-*c*) (Shelnutt et al., 1984). The Raman core-size (Spaulding et al., 1975; Spiro, 1982) and oxidation-state marker lines (Yamamoto et al., 1973; Spiro, 1982; Spiro & Strekas, 1974; Spiro & Burke, 1976) were found to be good indicators of the state of ligation (Shelnutt et al., 1984; Teraoka & Kitagawa, 1980). The marker lines are sensitive to the electronic structure changes in the porphyrin ring resulting from changes in the state of ligation at the metal (Shelnutt et al., 1984). In addition, the ^{Cu}cyt-*c* study used a new procedure (Shelnutt et al., 1984; Shelnutt, 1984; Shelnutt & Ortiz, 1985) based on the four-orbital model (Gouterman, 1959, 1978) and iterative extended Huckel molecular orbital calculations to determine the effects of ligation on the frontier π-orbitals of the porphyrin ring. The shifts in the frontier molecular orbitals and the predicted changes in the absorption spectrum based on these level shifts are also consistent with addition of an axial ligand.

We now report the use of resonance Raman difference spectroscopy (RDS) to investigate the state of coordination of Ni(II) in ^{Ni}Hb, ^{Ni}Mb, and a variety of model Ni–porphyrin compounds. The Raman results show that one site of the chromophores in ^{Ni}Hb contains four-coordinate Ni–protoporphyrin IX [Ni(ProtoP)] by analogy to Ni(ProtoP) in noncoordinating solvents. The other site in ^{Ni}Hb and the similar site in ^{Ni}Mb have very different Raman spectra from both four- and six-coordinate model Ni(ProtoP) complexes. The Raman data for the marker lines of the reconstituted proteins are consistent with five-coordination for the latter sites. Identification of the Ni–ligand stretching mode at 236 cm^{-1} by ^{64}Ni isotopic substitution is consistent with five-coordination and imidazole as the axial ligand. The five-coordinate complex of ^{Ni}Hb and ^{Ni}Mb is unique to the reconstituted proteins; no similar five-coordinate model Ni–porphyrins were found.

Materials and Methods

^{Ni}Hb and ^{64}Ni-reconstituted Hb were prepared according to reported methods (Alston et al., 1984). ^{Ni}Mb was made by the method of Alston & Storm (1979). Solutions of the proteins in 0.05 M phosphate buffer at pH 7.5 were used for obtaining spectra. The proteins are stable in air and do not photodecompose. Ni(ProtoP), Ni–uroporphyrin [Ni(UroP)], and Ni–octaethylporphyrin [Ni(OEP)] were obtained from Porphyrin Products and used without further purification. All solvents were of highest purity obtainable from commercial sources. Imidazole and 1,2-dimethylimidazole were distilled prior to use. All materials showed the literature UV–visible absorption spectra. Absorption spectra were obtained on a Perkin-Elmer Model 330 spectrophotometer.

Raman spectra were obtained on selected pairs of samples in a Raman difference spectrometer described previously (Shelnutt et al., 1979; Shelnutt, 1983a). The 90° scattering geometry was employed. Spectral resolution was 4 cm^{-1}. All spectra were obtained at room temperature. Samples were excited with a krypton ion laser (Coherent 3000K) using the 406.7- or 413.1-nm laser lines. To avoid heating, the samples were irradiated in a rotating (100-Hz) cell with two compartments. The laser power at the sample was about 250 mW in a partially defocused beam. The Ni porphyrins are very stable to visible light and even higher powers could be used. No sample decomposition was observed as determined by the lack of changes in successive scans of the Raman spectrum during signal averaging and in the absorption spectrum taken before and after the Raman spectrum.

Results

The UV–visible absorption spectrum of ^{Ni}Hb is shown in Figure 1a. For comparison, the spectrum of Ni(ProtoP) in neat pyridine is also given (Figure 1b). The most obvious feature in the spectra is the presence of a split Soret band. The blue component of the Soret is located near the usual frequency (25 000 cm^{-1}) of Ni(ProtoP) model compounds in noncoordinating solvents and cetyltrimethylammonium bromide (CTAB) micelles in aqueous solution. The red component of the Soret band of ^{Ni}Hb is shifted by about 1300 cm^{-1}; however, this shift is not as large and is outside the range of shifts expected for six-coordinate (vide infra) Ni porphyrins in coordinating solvents such as pyridine and pyrrolidine (1700 cm^{-1}). ^{Ni}Mb exhibits only the red-shifted Soret component. Further, after CPA digestion, ^{Ni}Hb also retains only the red Soret band (Manoharan et al., 1985).

In the Q-band region, the band near 17 900 cm^{-1} is at the position of the α-band of known (LaMar & Walker, 1978) four-coordinate Ni porphyrins. The low-energy shoulder is the α-band corresponding to the red-shifted Soret. Band maxima for other model Ni porphyrins are listed in Table I.

The large difference in frequency of the two Soret band maxima allows selective excitation of the Raman spectra of

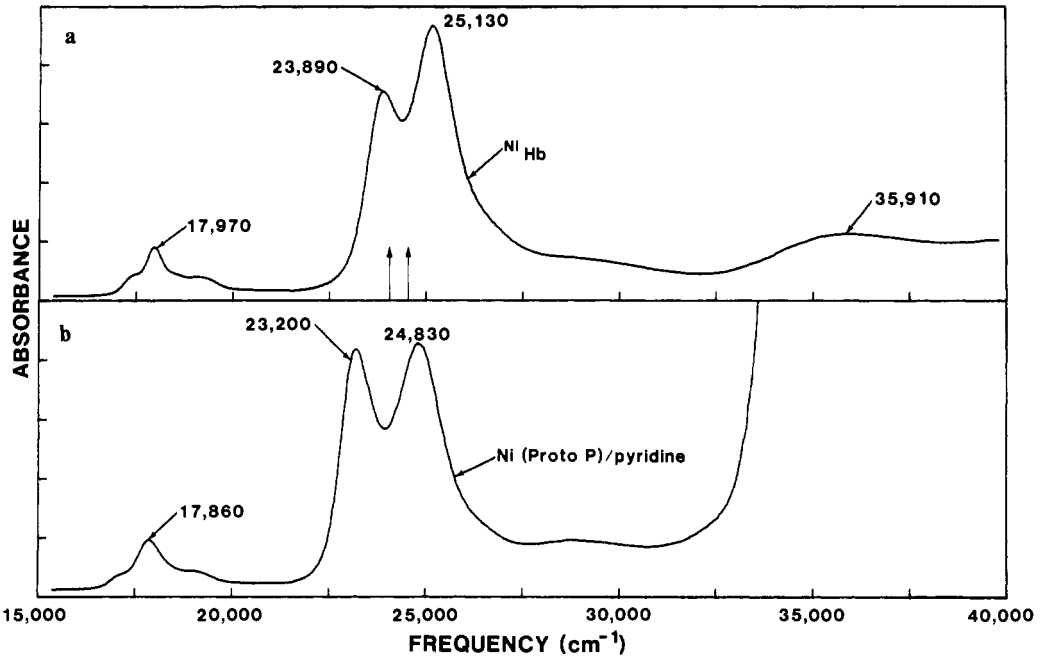

FIGURE 1: UV–visible absorption spectrum of nickel-reconstituted hemoglobin at pH 7.5 and the absorption spectrum of nickel protoporphyrin IX free acid in pyridine.

Table I: Absorption Band Maxima of Ni-Reconstituted Hemoglobin, Myoglobin, and Ni Porphyrins

coord no.	nickel porphyrin	solvent	band maxima (cm^{-1}) ν_{Soret}	ν_α	ν_β
4	Ni(ProtoP)	CTAB/base	~25 000	~17 860	~19 160
		sty/2-Vpy[a]	24 800	17 780	19 060
		1-MeIm	24 890	17 910	
		pyridine	24 830	17 860	
		pyrrolidine	~24 800		
	Ni(ProtoP)	copolymer[b]	24 980	17 820	19 120
	Ni(OEP)	pyridine	25 460	18 160	19 390
	^{Ni}Hb	P_i buffer	25 180	17 920	
6	Ni(ProtoP)	1-MeIm	23 110		
		pyridine	23 200	~17 000	
		pyrrolidine	23 120	17 050	18 070
	Ni(OEP)	pyridine	~23 750		
5	^{Ni}Hb	P_i buffer	23 870	~17 250	
	^{Ni}Mb	P_i buffer	23 940	17 140	~18 520

[a] Styrene/2-vinylpyridine. [b] Copolymer with styrene/2-vinylpyridine copolymer in toluene.

the chromophores in each of the two sites. With 406.7-nm excitation, the blue-shifted component is resonance-enhanced; with 413.1-nm excitation, the red-shifted chromophores are selectively enhanced. The Raman spectrum of ^{Ni}Hb at 413.1 nm is shown in Figure 2a, and Raman lines of two species are evident. Comparison with the 406.7 nm excited Raman spectrum in Figure 2b confirms that the lines labeled by the numeral 4 are enhanced by excitation of the blue Soret band; Raman lines labeled 5 are enhanced by excitation of the red Soret band.

The lines of ^{Ni}Hb indicated by 4's in Figure 2 are assigned to a four-coordinate Ni(ProtoP) site in the protein by comparison with four-coordinate models such as Ni(ProtoP) in CTAB micelles, whose spectrum is shown in Figure 2c. The frequencies of four of the Raman marker lines, ν_4, ν_3, ν_2, and ν_{10}, for ^{Ni}Hb and ^{Ni}Mb are given in Table II along with a number of four- and six-coordinate Ni–porphyrin models. The line at 1566 cm^{-1} in the four-coordinate models is ν_{38}, and the line at 1612 cm^{-1} is ν_{37}. Finally, the line at 1634 cm^{-1} is the vinyl C=C stretching mode of the four-coordinate form. The vinyl mode has different frequencies for four- and five- (or six-) coordinate species, and consequently, the lines may be too weak to be observed in ^{Ni}Hb, which is a mixture of the two forms. It is also possible that the vinyls have a special orientation with respect to the porphyrin-ring plane and that in this orientation the vinyl mode exhibits less resonance enhancement. The notation for the modes is that of Abe et al. (1978), and the assignments are in analogy with four-coordinate Ni–porphyrin model compounds (Abe et al., 1978; Choi et al., 1982).

In Figure 3, we give the Raman spectrum of ^{Ni}Mb and a model six-coordinate Ni(ProtoP) (in neat pyrrolidine). The spectra at first glance are somewhat similar. In particular, the Raman oxidation-state and core-size marker lines in both spectra are strongly shifted to low frequency compared with four-coordinate models. For example, ν_{10} shifts from 1658 cm^{-1} for Ni(ProtoP) in CTAB to 1617 cm^{-1} in pyrrolidine and 1620 cm^{-1} for ^{Ni}Mb and for the sites of ^{Ni}Hb possessing the red-shifted Soret. The oxidation-state marker line ν_4 is at 1365 cm^{-1} for Ni(ProtoP) in pyrrolidine and at 1368 cm^{-1} for ^{Ni}Mb but at 1378 cm^{-1} for four-coordinate Ni(ProtoP) in CTAB.

On the other hand, a closer inspection of the marker lines shows clear differences between ^{Ni}Mb and the six-coordinate models. For example, ν_2 for six-coordinate Ni(ProtoP)'s is in the range of 1560–1568 cm^{-1}, but ν_2 for ^{Ni}Mb is at 1572 and at 1573–1574 cm^{-1} for the coordinated site in ^{Ni}Hb. Similarly, ν_3 for the proteins is about 10 cm^{-1} higher than for the six-coordinate models (see Table II). In fact, closer inspection of ν_4 and ν_{10} frequencies show them also to be a bit high for the proteins.

Finally, Figure 4 shows the low-frequency Raman spectrum of ^{64}Ni-reconstituted hemoglobin and the spectrum of natural abundance ^{Ni}Hb. The spectra were obtained simultaneously on a Raman difference spectrometer so that accurate comparisons of line frequencies could be made. Excepting the line at 236 cm^{-1}, all of the lines in the spectrum of ^{Ni}Hb shift by less than 1 cm^{-1} to low frequency upon ^{64}Ni substitution. On the basis of the 6–7-cm^{-1} shift to low frequency, the 236-cm^{-1} line is assigned to the Ni–ligand stretch as discussed in the next section.

In the preceding discussion we have identified the paramagnetic Ni(ProtoP)–piperidine complex as six-coordinate on

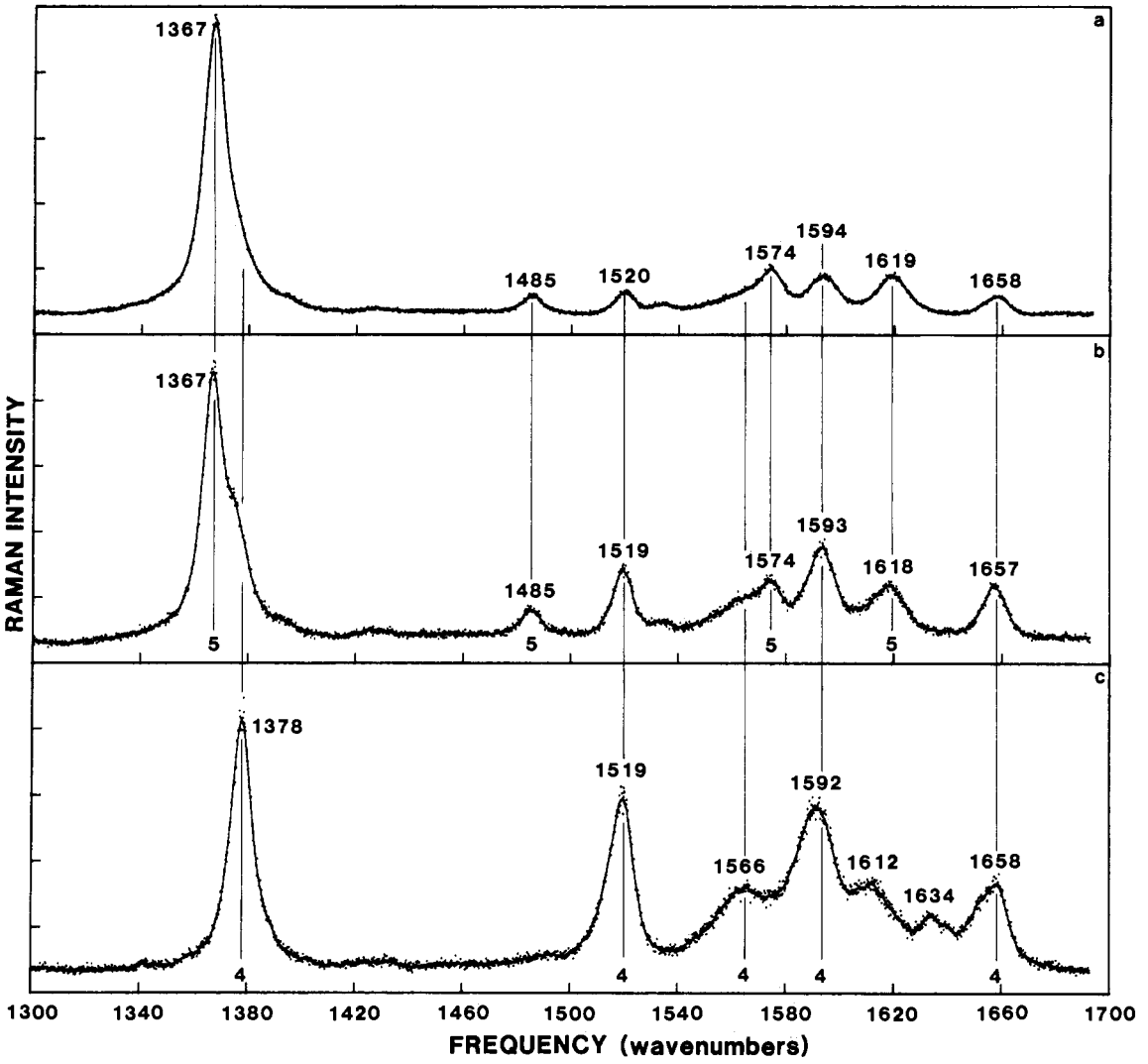

FIGURE 2: Raman spectra of nickel-reconstituted hemoglobin (pH 7.5) obtained with 413.1-nm excitation (a) and with 406.7-nm excitation (b) and the spectrum of nickel protoporphyrin IX free acid in cetyltrimethylammonium bromide micelles in 0.1 M NaOH (c). Spectra b and c were obtained simultaneously on the Raman difference spectrometer.

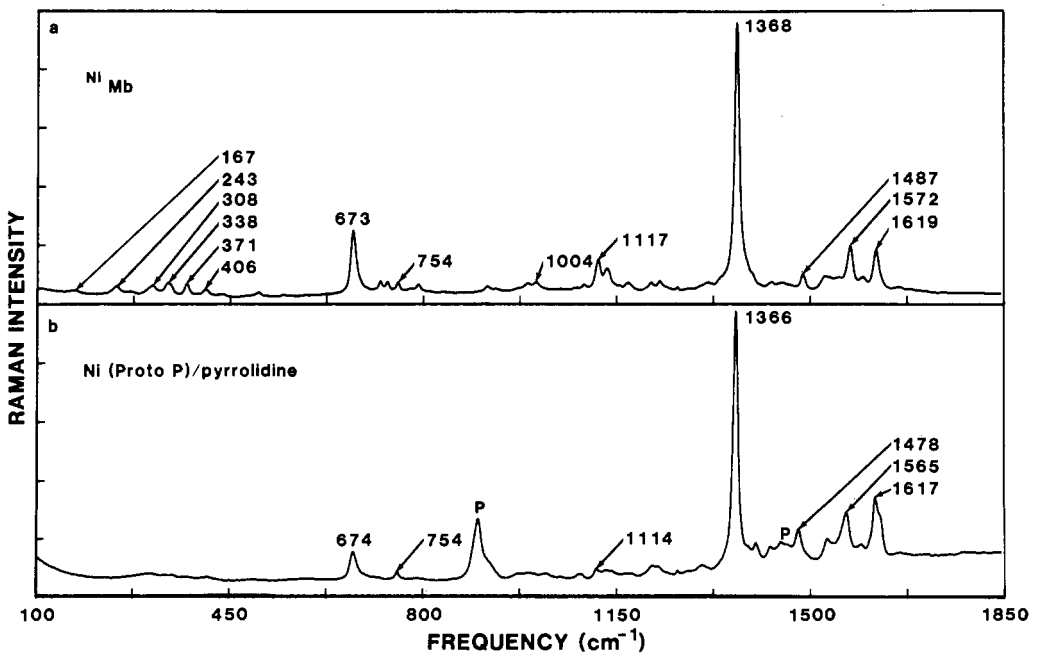

FIGURE 3: Raman spectra of nickel-reconstituted myoglobin (pH 7.5) (a) and nickel protoporphyrin IX in pyrrolidine (b). Some pyrrolidine lines are indicated (P). The spectra were obtained simultaneously; excitation is with the 413.1-nm line of a Kr^+ laser.

Table II: Frequencies of Raman Oxidation-State and Core-Size Marker Lines for Nickel Hemoglobin, Nickel Myoglobin, and Four- and Six-Coordinate Nickel Porphyrins

coord no.	nickel porphyrin	solvent	Raman marker line frequencies (cm^{-1})			
			ν_4	ν_3	ν_2	ν_{10}
4	Ni(ProtoP)	CTAB/base	1378	1519–1520	1592–1593	1657–1659
		sty/2-Vpy[b]	1377	1518		
		1-MeIm	~1377	1515	1588	1657
		1,2-Me_2Im	1376	~1516	1587–1588	1653–1655
		pyridine	1376	1518	1589	1655
		piperidine		~1520	1590	~1657
		pyrrolidine			1589	1658
	^{Ni}Hb	P_i buffer	1378	1519	1592–1594	1657–1658
	^{Ni}Mb[a]	P_i buffer			~1596	~1661
	Ni(ProtoP) polymers	film	1377–1380	1517–1520	1595–1598	1657
		copolymer	1377–1378	1517–1520	1591	1652–1659
	Ni(OEP)	CH_2Cl_2	1381	1519	1600	1655–1657
		CH_2Cl_2[c]	1383	1519	1602	1655
		CH_2Cl_2[d]	1382	1519	1600	
		pyridine	1379–1383	1517–1519	1598	1651–1657
		triclinic[d]	1382	1524		1660
		tetragonal[d]	1382	1512	1595	1641
	Ni(UroP)	0.1 M NaOH	1384	1521	1603	1659
6	Ni(ProtoP)	pyrrolidine	1364–1366	1475–1478	1563–1565	1616–1617
		piperidine	1364–1365	1476–1477	1564	1616–1617
		1-MeIm	1364	1477	1564	1615
		pyridine	1365–1366	~1479	~1568	1616
		1,2-Me_2Im	~1365		~1560	~1618
	Ni(OEP)	piperidine	1369–1370	1480–1482	1586–1589	~1618
		pyridine	1369–1370			~1618
5	^{Ni}Mb	P_i buffer	1368	1487–1488	1572–1573	1620
	^{Ni}Hb	P_i buffer	1368	1485	1573–1574	1618–1620

[a] Partially photodegraded. [b] Styrene/2-vinylpyridine. [c] Abe et al., 1978. [d] Crystal data from Spaulding et al., 1975.

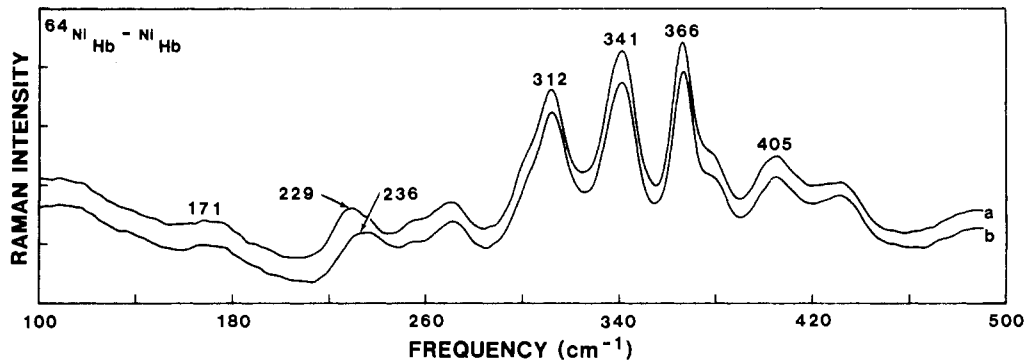

FIGURE 4: Low-frequency region of the Raman spectra of (a) ^{64}Ni-reconstituted hemoglobin A and (b) natural abundance Ni-reconstituted hemoglobin A at pH 7.5. Isotopic shifts are less than 1 cm^{-1} for all lines except the Ni–histidine mode at 236 cm^{-1}.

the basis of the nuclear magnetic resonance (NMR) and absorption studies of the Ni–tetraphenylporphyrin complexes by Walker and co-workers (Walker et al., 1975; LaMar & Walker, 1979). Although four- and six-coordinate forms are the predominant species in piperidine solution, both high- and low-spin five-coordinate forms are indirectly detected in the NMR work. In the Raman data for the model Ni porphyrins, we find little evidence of additional five-coordinate complexes; hence, either the five-coordinate forms must exist at low concentration, or else five-coordinate species must be nearly indistinguishable from the low-spin ($S = 0$) four-coordinate and the high-spin ($S = 1$) six-coordinate complexes. Weak evidence for an additional form is found for Ni(OEP) in CH_2Cl_2 and pyridine and for Ni(ProtoP) in pyridine and CTAB micelles (Figure 2c). In these solvents, ν_{10} exhibits a low-frequency shoulder near 1650 cm^{-1}. The shoulder does not appear for ν_{10} of the four-coordinate sites of ^{Ni}Hb.

Discussion

We first consider the high-frequency Raman marker lines. The Raman lines assigned (Abe et al., 1978; Choi et al., 1982) to the ν_3, ν_2, and ν_{10} in-plane vibrations of the porphyrin macrocycle correlate with the center to pyrrole nitrogen distance or core size for a variety of metalloporphyrins (Spaulding et al., 1975; Spiro, 1982). The Raman core-size marker lines are also sensitive to spin state (Yamamoto et al., 1973; Loehr & Loehr, 1973; Spiro, 1982; Spiro & Strekas, 1974; Spiro & Burke, 1976) and to axial ligation (Shelnutt et al., 1984; Teraoka & Kitagawa, 1980) at the metal ion in the central core of the ring. The sensitivity of the ring modes to core size is brought about by way of the metal's interaction with the electron of the macrocycle. The relationship between core size and marker-line frequencies logically must come about as a result of a core-size-dependent change in electronic structure if we are to explain the fact that the primary contribution to these normal modes is from the methine bridge motion and not a vibration involving nuclei of the ring bound directly to the metal, i.e., the pyrrole nitrogens.

Because ligation affects the metal's interaction with the porphyrin ring, it is not surprising that the core-size marker lines are also affected by addition of a ligand. In fact, for the nonhyper metalloporphyrins, the effect of ligation on the

π-system of the ring and the marker lines is not unlike the effect of metal substitution with a less electronegative (less covalent bond forming) metal (Shelnutt & Ondrias, 1984; Shelnutt & Dobry, 1983; Shelnutt, 1983b). The primary effect on the frontier π-orbitals of the ring upon addition of a fifth and/or sixth ligand is a shift in energy of the top-filled a_{2u} orbital (Shelnutt et al., 1984; Shelnutt & Ondrias, 1984; Shelnutt & Dobry, 1983; Shelnutt, 1983b). Direct interaction of the metal $4p_z$ orbital with the a_{2u} is allowed; none of the metal orbitals interact directly with the a_{1u} because it has nodes at the pyrrole nitrogens. The a_{2u} also places charge at the methine bridge carbons, providing a link with the marker line vibrations. Addition of a σ-donating ligand influences the metal–ring interaction by donating charges to the $4p_z$ orbital, raising its energy. As a result, the energy and charge of the a_{2u} is raised because the stabilizing interaction between the a_{2u} and $4p_z$ orbitals is weakened due to the larger gap between the two levels. Besides conjugation with the $4p_z$ orbital, a metal spin-state change caused by axial ligation may induce an additional change in core size.

A comparison of four-coordinate frequencies for the Raman marker lines with those for ^{Ni}Mb and the site with the red Soret band in ^{Ni}Hb shows that the shifts in frequency are those expected if a σ-donating axial ligand is added. The pattern of shifts occurring upon addition of a fifth ligand is one of large shifts to low frequency for the core-size marker lines and a somewhat smaller shift in the oxidation-state marker line ν_4, also to low frequency (Shelnutt et al., 1984; Shelnutt & Ondrias, 1984; Shelnutt & Dobry, 1983; Shelnutt, 1983b). Indeed, for ^{Ni}Hb and ^{Ni}Mb, the shift for ν_4 is only -11 cm^{-1} compared to shifts for ν_3, ν_2, and ν_{10} of -34, -20, and -40 cm^{-1}, respectively. A similar pattern of shifts is observed for addition of a fifth ligand in ^{Cu}cyt-*c* (Shelnutt et al., 1984).

Addition of a sixth ligand in the model Ni–porphyrin complexes apparently further lowers the frequencies of the Raman marker lines, although not to the same extent as adding the first axial ligand. The vibrations ν_3 and ν_2 show the largest additional shifts when a sixth ligand binds. The weakened effect of adding the second axial ligand is also noted in the smaller shift in the Soret band (400 cm^{-1} for the second vs. 1300 cm^{-1} for the first).

Molecular orbital calculations (Ake & Gouterman, 1970) predict a triplet $^3B_{1g}$ state for the five-coordinate site with the two holes for the Ni d^8 configuration occupying the d_{z^2} and $d_{x^2-y^2}$ orbitals (one each). The four-coordinate Ni site is most likely in the $^1A_{1g}$ state, for which the two holes are in the $d_{x^2-y^2}$ orbital and d_{z^2} is filled. The predicted Ni spin-state change is consistent with large changes in the core-size marker lines, since they are known to be sensitive to spin state in the Fe porphyrins. However, the spectral changes are partly a result of the strong axial ligation, since similar sized shifts occur upon addition of a ligand for vanadyl porphyrins and, in this d^1 configuration case, the spin state remains unchanged (Walker et al., 1975; Shelnutt & Dobry, 1983). It should be pointed out that electron paramagnetic resonance spectroscopy of the reconstituted proteins at liquid helium temperatures has failed to detect a high-spin Ni–porphyrin spectrum (Manoharan et al., 1985) and confirmation of the $S = 0$ state awaits magnetic susceptibility or NMR measurements.

As discussed above, the anomalous frequencies of the core-size marker lines of ^{Ni}Mb and the axially coordinated site in ^{Ni}Hb suggest that Ni has only one axial ligand. The ligand is guessed to be histidine on the basis of the apparently normal T structure of the reconstituted protein. That histidine is, indeed, the fifth ligand is further indicated by identification of the Ni–ligand stretching mode by ^{64}Ni isotopic substitution.

Raman difference spectroscopic comparison of the low-frequency (100–500-cm^{-1}) region of ^{Ni}Hb and the ^{64}Ni-reconstituted protein shows less than a 1-cm^{-1} shift in seven of the Raman lines in the region but a decrease of almost 7 cm^{-1} occurs for the line at 236 cm^{-1} (Figure 4). If the mode were a pure Ni–ligand vibration, then a 10-cm^{-1} decrease in frequency would have been predicted on the basis of the change in mass from 58.7 to 64. In analogy with iron hemoglobin and myoglobin, the mode is about 70% pure with other low-frequency modes having some Ni–$N_{pyrrole}$ content (Teroaka & Kitagawa, 1981; Argade et al., 1984), accounting for the slight lowering of some of their frequencies as well.

Imidazole of the proximal histidine is implicated by the frequency of the Ni–ligand stretch. It comes in the region (190–275 cm^{-1}) of Fe–histidine stretching frequencies in heme proteins and model Fe–porphyrin complexes (Ondrias et al., 1982; Teroaka & Kitagawa, 1981).

One might have expected a much lower frequency for the Ni–histidine stretch, ν(Ni–His), than for the Fe–histidine stretching mode of hemoglobin, because the binding of histidine to Ni is less stable. The clearest indication of the low affinity of histidine for Ni in ^{Ni}Hb is that an equilibrium between four- and five-coordinate species exist at room temperature. This is not the case for Fe hemoglobin. The weak binding is also reflected by the solution studies, which show a mixture of four- and six-coordinate forms at room temperature for the nickel–porphyrin complexes but not the corresponding iron–porphyrin complexes. At first glance, the high frequency for ν(Ni–his) is disturbing in light of the low binding energy. However, one must also consider contributions to the binding energy other than from just the Ni–histidine bond. For example, the decrease of up to 40 cm^{-1} in the core-size marker lines indicates (1) that the energy of the porphyrin ring is destabilized by addition of the ligand and (2) that the porphyrin–Ni bond is weakened. The weakening of the porphyrin–Ni bond is deduced from the about 0.08-Å expansion of the porphyrin core (center to pyrrole nitrogen distance) calculated from the change in the core-size marker line frequencies. The calculated core expansion is the same that is found in the X-ray crystal structures (Kirner et al., 1975). Thus, the strong Ni–histidine bond is somewhat compensated for energetically by the weakening of the porphyrin–Ni bond. This weakening is caused by the energy required for promotion of an electron from the d_{z^2} orbital to the antibonding $d_{x^2-y^2}$ orbital that points toward the pyrrole nitrogens. The net effect is a low affinity of histidine for Ni.

It is interesting to make an R–T comparison of the Ni–histidine vibrational frequency. For Fe hemoglobins, an R–T shift of between 3 and 8 cm^{-1} is noted for the deoxy proteins, the exact shift depending on the R-like protein chosen for the comparison. Myoglobin has the high-affinity R-like tertiary structure, so a comparison of the Ni–histidine Raman line in ^{Ni}Hb and ^{Ni}Mb gives an estimate of the T $\rightarrow$ R shift for the Ni-reconstituted hemoglobin.

The assignment of a line of ^{Ni}Mb near 243 cm^{-1} to ν(Ni–His) seems simple because each low-frequency line in the ^{Ni}Hb spectrum can be easily matched with a corresponding line in ^{Ni}Mb. This assignment is deceptive, however, as shown by isotopic substitution in ^{Ni}Mb (J. A. Shelnutt, N.-T. Yu, and K. Alston, unpublished results). A Raman line of the porphyrin moiety also occurs at about 243 cm^{-1}, and apparently, the line is much stronger in ^{Ni}Mb than in ^{Ni}Hb, especially for Raman spectra obtained at 413.1-nm excitation. At 415.4 nm, however, the 243-cm^{-1} line is weaker relative to the Ni–

histidine stretch and occurs about 1 cm^{-1} lower because of overlap with the lower frequency Ni–histidine mode. This interpretation of the 200–300-cm^{-1} region is consistent with the isotopic substitution data for ^{Ni}Mb. ^{64}Ni-reconstituted myoglobin exhibits (1) reduced intensity in the 243-cm^{-1} region, (2) a 2-cm^{-1} decrease in frequency of the porphyrin mode, and (3) the apperance of a shoulder at about 233 cm^{-1}. These isotopic substitution results suggest that the Ni–histidine mode in ^{Ni}Mb occurs near 241 cm^{-1} and shifts to about 233 cm^{-1} upon ^{64}Ni substitution. The isotope shift is about 8 ± 2 cm^{-1}. In addition, the degenerate porphyrin mode at 243 cm^{-1} is also slightly metal sensitive, suggesting the presence of some $N_{pyrrole}$ character.

The Ni isotopic substitution results closely parallel the isotopic substitution data for native iron myoglobin (Argade et al., 1984). ^{64}Ni substitution in myoglobin also causes a weak line near 270 cm^{-1} to shift to about 261 cm^{-1}. The Raman difference spectrum shows that the largest isotope effect (largest change in difference intensity) is in the 240-cm^{-1} region however, not the 265-cm^{-1} region. Because the isotope shifts in both the 241- and 270-cm^{-1} lines is large, both are almost pure Ni–ligand stretches. This suggests that the additional isotope-sensitive line in myoglobin at 270 cm^{-1} results from a fraction of the protein molecules with an even stronger Ni–histidine bond. Alternatively, a pure metal–$N_{pyrrole}$ mode is possibly observed.

For the predominate form in ^{Ni}Mb, the Ni–histidine stretching mode occurs near 241 cm^{-1}. Further, the 241-cm^{-1} value gives a 5-cm^{-1} increase for the R-like structure. This value is in line with the 3–8 cm^{-1} T → R increase observed for Fe hemoglobins.

In some respects, it is surprising that the R–T shift of the Ni–histidine mode is observed at all. One might have expected that the change in structure would only affect the ratio of the number of four- and five-coordinate sites in the protein and not affect the structure of the five-coordinate sites themselves. The Raman data show that this is not the case. In myoglobin, the R-like environment of the chromophore favors more strongly bonded histidine. The stronger axial ligand bond apparently tilts the equilibrium in favor of the five-coordinate form. This interpretation is consistent with the conclusion of Manoharan et al. (1985) that five-coordinate sites are not localized to either the α- or the β-chains but that an equilibrium distribution of sites in both chains is likely.

Finally, we have measured the difference in frequency of the oxidation-state marker line ν_4 for ^{Ni}Hb and ^{Ni}Mb. In R–T comparisons for Fe hemoglobins, ν_4 decreases for the R structure by up to 1.5 cm^{-1} (Ondrias et al., 1982). Further, the shift in ν_4 anticorrelates with the shift in the Fe–histidine mode (slope = −5). This relationship should be contrasted with that observed for ferrous horseradish peroxidase (HRP) for which a positive correlation between the frequencies is observed (slope = 9) (Shelnutt et al., 1986). If one of these two relationships holds for ν_4 and the Ni–histidine vibration of ^{Ni}Hb, then we would predict either a ($^5/_5$=) 1.0-cm^{-1} *decreases* (Hb-type relationship) or a ($^5/_9$=) 0.6-cm^{-1} *increase* (HRP-type relationship) in ν_4 for ^{Ni}Mb relative to ^{Ni}Hb on the basis of the 5-cm^{-1} increase in the Ni–histidine mode. We actually observe an *increase* of 0.34 ± 0.07 cm^{-1} for ν_4. This observation would favor a HRP-type instead of a Hb-type relationship, providing that similar shifts are found for other ^{Ni}Hb R–T comparisons. Other high-frequency marker lines exhibit R–T differences including ν_3 (1.7 ± 0.6 cm^{-1}, higher for ^{Ni}Mb), ν_2 (1.0 ± 0.4 cm^{-1}, lower for ^{Ni}Mb), and ν_{10} (0.4 ± 0.4 cm^{-1}, lower for ^{Ni}Mb). Among the various human Fe hemoglobins, all of the marker lines shift to low frequency for the R-like structures. However, in a comparison of hemoglobin and sperm whale myoglobin, this pattern of shifts is not observed (ν_3 and ν_{10} do not shift) (Ondrias et al., 1982). Until further R–T comparisons for Ni-reconstituted hemoglobins are in hand, the meaning of the shifts in the marker lines will not be resolved.

Ni(II)-reconstituted hemoglobins and myoglobins represent unique models for investigating R–T conformational changes. Further characterization of their Raman spectra is needed to understand the dual roles of the metal ion and the porphyrin in the mechanism of O_2 affinity control in these heme proteins.

Registry No. Ni(ProtoP), 15415-30-2; Ni(UroP), 84098-84-0; Ni(OEP), 24803-99-4; Ni, 7440-02-0; ^{64}Ni, 14378-31-5; histidine, 71-00-1.

REFERENCES

Abe, M., Kitagawa, T., & Kyogoku, Y. (1978) *J. Chem. Phys. 69*, 4526–4534.

Ake, R. L., & Gouterman, M. (1970) *Theor. Chim. Acta 17*, 408.

Alston, K., & Storm, C. B. (1979) *Biochemistry 18*, 4292–4300.

Alston, K., Dean, A., & Schechter, A. N. (1980) *Mol. Immunol. 17*, 1475.

Alston, K., Friedman, F. K., & Schechter, A. N. (1982) *Hemoglobin 6*, 15.

Alston, K., Schechter, A. N., Arcoleo, J. P., Greer, J., Parr, G. R., & Friedman, F. K. (1984) *Hemoglobin 8*, 47.

Alston, K., Park, C. M., Rodgers, D. W., Edelstein, S. J., & Nagel, R. L. (1985) *Blood 64* (Part 2), 556–558.

Argade, P. V., Sassaroli, M., Rousseau, D. L., Inubushi, T., Ikeda-Saito, M., & Lapidot, A. (1984) *J. Am. Chem. Soc. 106*, 6593–6596.

Choi, S., Spiro, T. G., Langry, K. C., & Smith, K. M. (1982) *J. Am. Chem. Soc. 104*, 4337–4344.

Flatmark, T., & Robinson, A. B. (1968) *Structure and Function of Cytochromes* (Okunuki, K., Daman, M. D., & Sekuzu, I., Eds.) p 318, University Park Press, Baltimore, MD.

Gouterman, M. (1959) *J. Chem. Phys. 30*, 1139.

Gouterman, M. (1978) *Porphyrins 3*, 1.

Hoffman, B. M. (1979) *Porphyrins 7*, 403.

Kirner, J. F., Garofalo, J., Jr., & Scheidt, W. R. (1975) *Inorg. Nucl. Chem. Lett. 11*, 107–112.

LaMar, G. N., & Walker, F. A. (1979) *Porphyrins 4*, 61.

Loehr, T. M., & Loehr, J. S. (1973) *Biochem. Biophys. Res. Commun. 55*, 218–223.

Manoharan, P. T., Alston, K., & Rifkind, J. M. (1983) *Bull. Magn. Reson. 5*, 255.

Manoharan, P. T., Alston, K., & Rifkind, J. M. (1985) *Biochemical and Inorganic Aspects of Copper Coordination Chemistry* (Karlin, K. D., & Zubieta, J., Eds.) Academic Press, New York (in press).

Ondrias, M. R., Rousseau, D. L., Shelnutt, J. A., & Simon, S. R. (1982) *Biochemistry 21*, 3428–3437.

Shelnutt, J. A. (1983a) *J. Phys. Chem. 87*, 605–616.

Shelnutt, J. A. (1983b) *J. Am. Chem. Soc. 105*, 774–778.

Shelnutt, J. A. (1984a) *J. Phys. Chem. 88*, 4988–4992.

Shelnutt, J. A. (1984b) *J. Phys. Chem. 88*, 6121–6127.

Shelnutt, J. A., & Dobry, M. M. (1983) *J. Phys. Chem. 87*, 3012–3015.

Shelnutt, J. A., & Ondrias, M. R. (1984) *Inorg. Chem. 23*, 1175–1177.

Shelnutt, J. A., & Ortiz, V. (1985) *J. Phys. Chem. 89*, 4733–4739.

Shelnutt, J. A., Rousseau, D. L., Dethmers, J. K., & Margoliash, E. (1979) *Proc. Natl. Acad. Sci. U.S.A. 76*, 4409–4413.
Shelnutt, J. A., Straub, K. D., Rentzepis, P. M., Gouterman, M., & Davidson, E. R. (1984) *Biochemistry 23*, 3946–3954.
Shelnutt, J. A., Alden, R. G., & Ondrias, M. R. (1986) *J. Biol. Chem.* (in press).
Spaulding, L. D., Chang, C. C., Yu, N.-T., & Felton, R. H. (1975) *J. Am. Chem. Soc. 97*, 2517–2525.
Spiro, T. G. (1982) in *Iron Porphyrins* (Lever, A. B. P., & Gray, H. B., Eds.) Part II, p 89, Addison-Wesley, Reading, MA.
Spiro, T. G., & Strekas, T. C. (1974) *J. Am. Chem. Soc. 96*, 338–345.
Spiro, T. G., & Burke, J. M. (1976) *J. Am. Chem. Soc. 98*, 5482–5489.
Teroaka, J., & Kitagawa, T. (1980) *J. Phys. Chem. 84*, 1928–1935.
Teroaka, J., & Kitagawa, T. (1981) *J. Biol. Chem. 256*, 3969–3977.
Walker, F. A., Hui, E., & Walker, J. M. (1975) *J. Am. Chem. Soc. 97*, 2390–2397.
Yamamoto, T., Palmer, G., Gill, D., Salmeen, I. T., & Rimai, L. (1973) *J. Biol. Chem. 248*, 5211–5213.

A New Trophoblast-Derived Growth Factor from Human Placenta: Purification and Receptor Identification†

Anis Sen-Majumdar, Uma Murthy, and Manjusri Das*
Department of Biochemistry and Biophysics, University of Pennsylvania School of Medicine, Philadelphia, Pennsylvania 19104
Received August 1, 1985

ABSTRACT: This paper describes the identification and characterization of a new peptide growth factor. The peptide was isolated from trophoblastic brush border membranes of human placenta. The purified preparation was homogeneous and consisted of a single polypeptide of M_r 34 000 with a p*I* of about 6.0. This peptide stimulated DNA replication in cultured fibroblasts. The following association was seen between activity and protein: (a) During DEAE-cellulose chromatography, both the 34-kilodalton (kDa) protein and the mitogenic activity displayed identical binding and salt dependence of elution. (b) Nondenaturing electrophoresis at pH 8.3 revealed a comigration of the 34-kDa protein and the DNA replication stimulatory activity. (c) Identical electrophoretic mobilities were displayed for both activity and protein at pH 7.0. These results demonstrate that the preparation is homogeneous and show that growth factor activity is intrinsic to the 34-kDa polypeptide. Binding of the ^{125}I-labeled 34-kDa mitogen to target fibroblastic cells was specific; i.e., nanomolar concentrations of the unlabeled 34-kDa protein competed effectively with the labeled protein, whereas a variety of well-characterized growth factors and hormones were unable to compete even at micromolar levels. Thus the 34-kDa protein interacts with target cells through highly specific surface receptors. Chemical cross-linking techniques were used to investigate the identity of the receptor for the 34-kDa mitogen. Cross-linking of fibroblastic cells containing bound ^{125}I-labeled 34-kDa protein generated a radiolabeled complex of 86 kDa in all four different cell types examined. The amount of labeled complex formed decreased drastically in the presence of excess unlabeled 34-kDa protein but was unaffected in the presence of other growth factors. The results suggest that the binding of the placental mitogen to target cells is mediated through a 50-kDa surface protein which may represent the whole receptor or only the binding subunit of an oligomeric receptor. In its molecular weight and binding specificity, this "mitogen receptor" is different from the well-characterized receptors for epidermal growth factor, platelet-derived growth factor, insulin-like growth factor, or β-transforming growth factor. Implications of these findings and the teleological significance of the membranous growth factor are discussed.

Growth factors and their receptors play a central role in the control of cell proliferation. Demonstration in recent years of structural and functional homologies between these normal growth control molecules and those responsible for cell transformation adds considerable interest to studies on these proteins (Waterfield et al., 1983; Downward et al., 1984). Four important classes of polypeptide growth factors have been identified, and their interactions with cell-surface receptors have been well characterized. These are the following: (a) epidermal growth factor (EGF)[1] and EGF-like factors, a family of 6000–7000-dalton polypeptides that share a common receptor that shows homology with the *erb-B* oncogene product (Cohen, 1962; Das, 1982; Downward et al., 1984; Tam et al., 1984); (b) platelet-derived growth factor (PDGF), a 25 000–30 000-dalton protein that shows identity with the *sis* oncogene product (Waterfield et al., 1983; Doolittle et al., 1983); (c) insulin and insulin-like growth factors, a class of structurally related 6000–7000-dalton proteins that interact with multiple

†Supported by NIH Research Grants AM-25819 and HD-17896 to M.D.

[1] Abbreviations: EGF, epidermal growth factor; PDGF, platelet-derived growth factor; IGF, insulin-like growth factor; β-TGF, β-transforming growth factor; Il-2, interleukin 2; LHRH, luteinizing hormone releasing hormone; BS^3, bis(sulfosuccinimido) suberate; DTSSP, bis(sulfosuccinimido) 3,3′-dithiobis(propionate); DME medium, Dulbecco's modified Eagle's medium; FBS, fetal bovine serum; EBSS, Earle's balanced salt solution; PBS, phosphate-buffered saline; SDS, sodium dodecyl sulfate; βME, β-mercaptoethanol; BSA, bovine serum albumin; Hepes, 4-(2-hydroxyethyl)-1-piperazineethanesulfonic acid; Tris, tris(hydroxymethyl)aminomethane.

0006-2960/86/0425-0627$01.50/0